International Journal of
Advances in Scientific Research and Engineering (ijasre)

E-ISSN : 2454-8006

DOI: 10.31695/IJASRE.2020.33698

Volume 6, Issue 1
January - 2020

Performance Investigation of Evacuated Tube Collector using Different Nano fluids Applied to Winter Climatic Conditions in Egypt

AbdallaGomaa, Fifi N. M. Elwekeel , Mahmoud Abdelmagied & Momen I. Radwan

Department of Refrigeration and Air-Conditioning Technology

Faculty of Industrial Education

Helwan University, 11282 Cairo, Egypt

ABSTRACT

In this paper, the performance of the evacuated tube solar collector is investigated theoretically by the TRNSYS program. The simulation is conducted during the winter of 14th February-2019 in Cairo – Egypt. In this simulation, water and Nanofluids are working fluids. The types of Nanofluids are CeO2/water, WO3/water and AL2O3/water. The simulation is conducted at0.015%, 0.025%, 0.035% and 0.045% (volume concentrations).The mass flux rate and tilt angle are 0.017 kg/s.m2and 45o; respectively. The results show that the collector has the highest performance using nanofluids at studied concentrations. At 12:00 PM, the highest useful energy gain can be obtained from CeO2/water Nanofluid at 0.045% concentration, while thermal efficiency is higher by 34.2% than water. The nanofluidWO3/water presents low performance than that of CeO2/water and AL2O3/water. The thermal efficiencies ofAL2O3/ water and WO3/ water Nanofluids are higher than water by 28.4% and 12.5%; respectively, at concentration of 0.045% and 12:00PM.

Key words: Evacuated Tube Collector, TRNSYS, Nano fluid.

NOMENCLATURE

A	Collector aperture area	[m^2]	**Subscripts**	
Cp	Specific heat capacity	[J/kg/k]	a	absorbed
F_R	Heat removal factor	[-]	amb	ambient
I	Solar radiation intensity	[W/m^2]	bf	Base fluid
k	Thermal conductivity	[W/m.K]	c	Collector
$\dot{Q}$	Heat energy	[kg/s]	f	Fluid
T	Temperature	[W]	i	Inlet
U	Overall heat losses coefficient	[W]	o	Outlet
		[W]	L	Losses
Greek Letters		[^{o}C]	hl	Heat losses
τ	Transmittance	[-]	nf	Nanofluid
α	Absorptance	[-]	np	Nano-particles
η	Efficiency of collector	[%]	rad	Radiation
ρ	Density	[kg/m^3]	u	useful

φ	concentration of nano-particles	[-]

Abbreviations

ETC	Evacuated Tube Collector	TRNSYS	Transient Systems Simulation
CeO_3	Cerium Oxide Nano-particles	WO_3	Tungsten trioxide Nano-particles
AL_2O_3	Aluminum Oxide Nano-particles		

1. INTRODUCTION

There are many studies available in literature for solar heating and cooling system simulation by means of transient system simulation software (TRNSYS). In this section, the survey focused on the researches related to TRNSYS simulation of solar heating and cooling systems starting with *Buonomo et al.* [1] presented TRNSYS simulation study for solar cooling system for peak energy consuming according to Italy conditions. The solar cooling system analyzed using base water and AL_2O_3 water nanofluid. *Fathima et al.* [2] conducted study for the performance analysis of evacuated tube solar collector using TRNSYS modeling with different nanofluidssuch as AL_2O_3, Silica, copper, carbon nanotube and aluminum. Solar cooling system with absorption chiller simulated by *Asim et al.* [3] using TRNSYS. Absorption chiller was powered by hot water from evacuated tube collector during system simulation. *Ayompe et al.* [4] performed a comparison between flat plate collector and evacuated tube collector by means of TRNSYS, type 73 used to model flat plate collector and type 538 for evacuated tube collector. The results showed that the useful energy delivered by evacuated tube collector was higher than that of flat plate collector. *Yang et al.* [5] established paper for thermal performance of solar heating system using TRNSYS simulation. Analysis included inlet and outlet temperatures of the collector, temperature distribution through storage tank and collector efficiency. *Fan et al*. [6] developed different TRNSYS models for evacuated tube heat pipe solar collector. First model was with flat fins and the other was with curved fins. *Abdunnabi and Loveday* [7] performed TRNSYS optimization analysis for two new models of thermosyphon solar collector compared with standard model. They concluded that the modified models gave a good agreement with the standard one and can be used to simulate the thermosyphon systems. *Mohammed et al.* [8] reported TRNSYS simulation for solar water heating system works with 10 m^2 flat plate collector to provide a hot water for 25 persons. The system was provided with auxiliary heater and the solar fraction of the system obtained by 69%. The maximum auxiliary energy needed for the system was during December month according to Baghdad, Iraq conditions. Different concentration levels for evacuated tube solar collector are simulated using TRNSYS modeling by *Ali et al*. [9]. The research determined that higher performance can be obtained at higher concentration levels. *Mohasseb* and *Kasaeian*[10] presented a comparison study between evacuated tube and flat plate solar collectors. The comparison simulated by means of TRNSYS program using Type 1b for flat plate and Type 71 for evacuated tube collector. The research concluded that the evacuated tube collector is better than the flat plate collector for both hot and cold climate conditions. *Utham et al.* [11] simulated the performance a solar cooling system according to India climate conditions. TRNSYS simulation included the optimization of storage tank volume, collector tilt angle and solar collector area. *Assilzadeh et al*. [12] developed a TRNSYS model for solar driven LiBr – H_2O absorption chiller in Malaysia, the results reported that the optimum solar collector area, storage tank volume and collector slope are 35m^2, 0.8m^3 and 22^o; respectively for 3.5 kW of chiller capacity. *Gill and Fung* [13] presented a study for solar heating system simulation for green house in Toronto, Canada. The results concluded that the solar heating system with gray water heat recovery system saves up to 80% of energy consuming. A new TRNSYS model for thermosyphon flat plat collector was developed by *Kalogirou et al.* [14]. Type 99 as new model was used instead of standard TRNSYS model of Type 45a, the results showed a good agreement between the data collected by Type 99 and the experimental work. *Abdunnabi et al*. [15] analyzed solar water heating system using TRNSYS program and validation of the system experimentally to measure the effectiveness of software. Different configuration of forced circulation of solar collector was investigated. The results reported that there was discrepancy between the experimental and the simulation due to the position of controlling sensor of circulating pump. *Cao et al* [16] performed TRNSYS simulation for solar water heating system according to real conditions. Various measured parameters were investigated by simulation such collector outlet water temperature, storage tank temperature and auxiliary heating.

Much researchers developed TRNSYS simulation for solar heating and cooling systems but the numerical studies of performance of solar collector using nanofluids are few. Also, the study of the performance of the evacuated solar collector(ETC) in the winter of Cairo - Egypt is not studied.So, in this work will be investigated the behavior of solar heating systemat winter climatic conditions of Cairo -Egypt. This study is conducted for different types of nanofluids and various concentrations.

DOI: 10.31695/IJASRE.2020.33698

2. METHODOLOGY

2.1 System modeling

The performance of evacuated solar collector is investigated by TRNSYS 17 [17], the system components are selected from the program library. The mathematical model for each component is formulated by FORTRAN code. In the present work Fig. 1 presents the TRNSYS model of solar heating system, according to this figure the model consists of standard evacuated tube collector TYPE 71, storage tank TYPE 60c, dual pipe fan coils TYPE 600, differential temperature controller TYPE 2b, weather data processor TYPE 15-6 TM2 according to weather conditions in Cairo – Egypt, TYPE 114 single speed pump for circulation of the working fluid, TYPE 14h used to adjust the pump operation schedule, the operation time is adjusted from 8:00 AM to 5:00 PM and the resulting data file is plotted by TYPE 65.

The evacuated solar collector ETCis the main component of the solar system, which has different parameters.

Table [1]TRNSYS input parameters for evacuated tube collector

Parameter	Value	Units
Number of collector in series	1	--
Collector aperture area (A_c)	1.59	m^2
Fluid specific heat	4.18	kJ/kg.K
Flow rate at test condition	0.017	$Kg/s.m^2$
Intercept efficiency	0.55	--
Negative 1st order efficiency coefficient	12	$kJ/hr.m^2.K$
Negative 2nd order efficiency coefficient	0.036	$kJ/hr.m^2.K$
Collector slope	45	Degrees

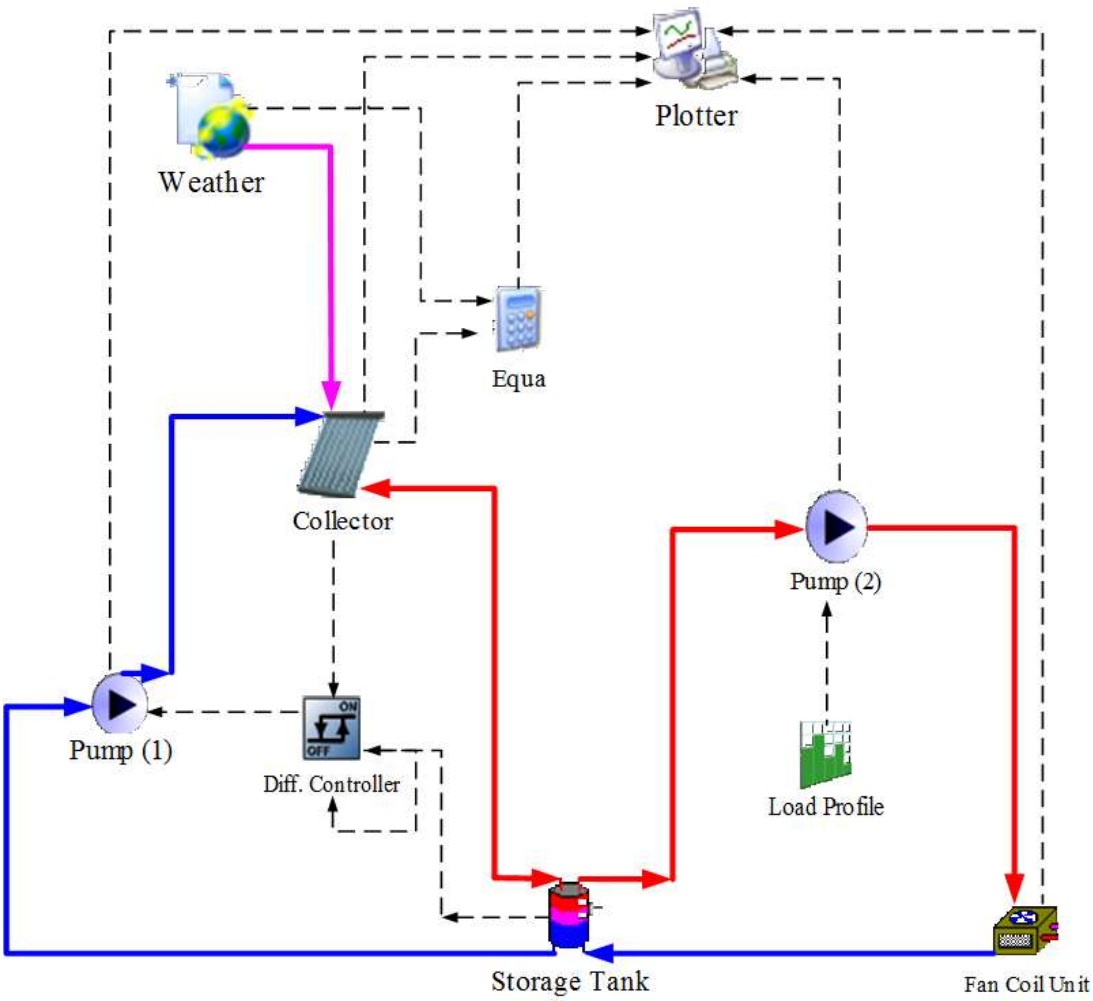

Fig. 1 TRNSYS model block diagram for solar heating system

DOI: 10.31695/IJASRE.2020.33698

2.2 Governing Equations

TRNSYS mathematical model and governing equations are as the following:

$$\dot{Q}_u = \dot{Q}_a - \dot{Q}_{hl} \tag{1}$$

$$\dot{Q}_{hl} = \dot{Q}_{Rad.L} + \dot{Q}_{Conv.L} + \dot{Q}_{Cond.L} \tag{2}$$

$$\dot{Q}_u = \dot{m}_f Cp_f \left(T_{f,o} - T_{f,i}\right) \tag{3}$$

The collector efficiency can be calculated by;

$$\eta_{c.} = \frac{\dot{m}_f Cp_f \left(T_{f,o} - T_{f,i}\right)}{I_{rad}.A_{coll.}} \tag{4}$$

$$= F_R\left(\tau\alpha\right) - F_R U_L\left(\frac{\Delta T}{I_{rad}}\right) - F_R U_L\left(\frac{\Delta T}{I_{rad}}\right)^2 \tag{5}$$

$$\eta_c = a_0 - a_1\left(\frac{T_{f,i} - T_{amb}}{I_{rad}}\right) \tag{6}$$

Where a_0 and a_1 are constants of collector efficiency. These constants are changed according to the operating conditions. These parameters are specified in Table [1].

The physical properties of nanofluid which are density (ρ), specific heat capacity (C_p) and thermal conductivity (k) are calculated as the following equations:

$$\rho_{nf} = \rho_{np}\left(\varphi\right) + \rho_{bf}\left(1-\varphi\right) \tag{7}$$

$$Cp_{nf} = \frac{(\rho Cp)_{np}(\varphi) + (\rho Cp)_{bf}(1-\varphi)}{(\varphi)\rho_{np} + \rho_{bf}(1-\varphi)} \tag{8}$$

$$k_{nf} = k_{bf}\,(1 + 8.733\varphi) \tag{9}$$

3. RESULTS AND DISCUSSIONS

The simulation is performed with different nanofluids. The nanofluids are CeO_2, WO_3 and AL_2O_3. CeO_2 and WO_3nanofluids are simulated according to *Sharafeldin* and *GyulaGrof* [18-19] while AL_2O_3 nanofluid is simulated according to *Javad and Sidik* [20]. From these studies, the efficiency constantsare shown in Table [2] at mass flux rate 0.017 kg/m^2 s.

Table [2] Efficiency constants for CeO_2, WO_3 and AL_2O_3nanofluids, [18-20]

Nanofluid type	Volume concentration	Efficiency Parameters	
		a_0	a_1
CeO_2nanofluid	0.015%	0.660	16.227
	0.025%	0.712	17.785
	0.035%	0.743	20.855
	0.045%	0.752	25.432
WO_3nanofluid	0.015%	0.664	26.751
	0.025%	0.685	32.073
	0.035%	0.709	33.952
	0.045%	0.736	32.387
AL_2O_3nanofluid	0.015%	0.386	1.567
	0.025%	0.427	1.668
	0.035%	0.467	1.768
	0.045%	0.508	1.868

DOI: 10.31695/IJASRE.2020.33698

3.1. Work Validation

Figures 2 and 3 show a comparison between prediction and experimental results. The validation uses CeO2/water and WO3/water as working fluids[18-19]. The comparison applied at mass flux rate of 0.017 kg/s.m^2, collector area of 1.59m^2. The concentrations of CeO_2/water and WO_3/water are 0.035% and 0.042%; respectively. Fig. 1 shows the thermal optical efficiency $F_R(\tau\alpha)$ of ETC using CeO_2/water nanofluid, the predicted thermal optical efficiency is recorded 0.752 while the experimentally value is 0.743. The predicted energy losses coefficient ($-F_R.U_L$) increases by about 5.8% than that of experimental.

Fig. 2 shows the thermal optical efficiency $F_R(\tau\alpha)$ and energy losses coefficient of ETC with WO3/water. The prediction result of thermal optical efficiency and energy losses coefficient are decreases by 3.9% and 12.7%; respectively, than experimental results. So, can be seen that a good agreement between the TRNSYS results and the experimental results.

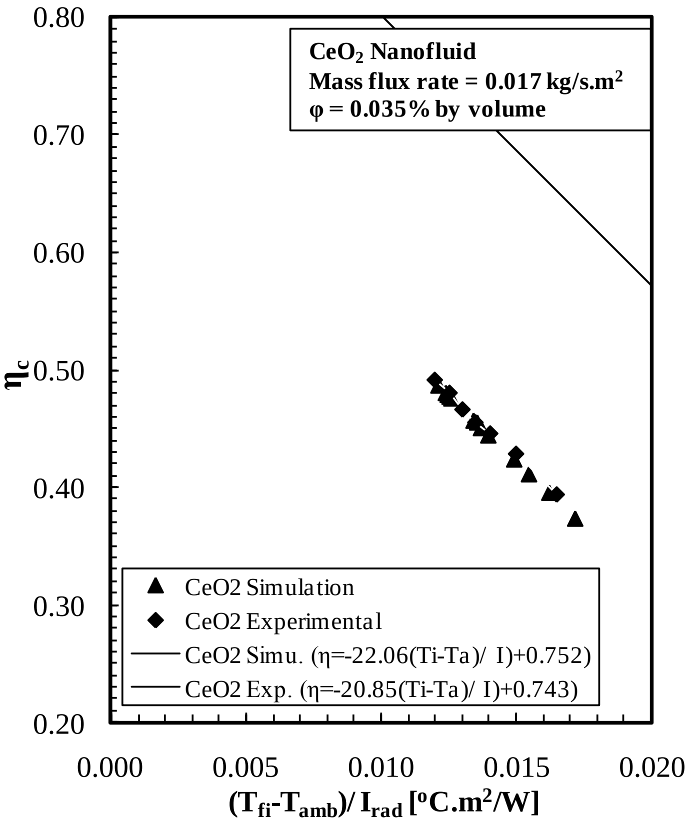

Fig. 1 Comparison between simulation results and experimental work for CeO_2 water nanofluid

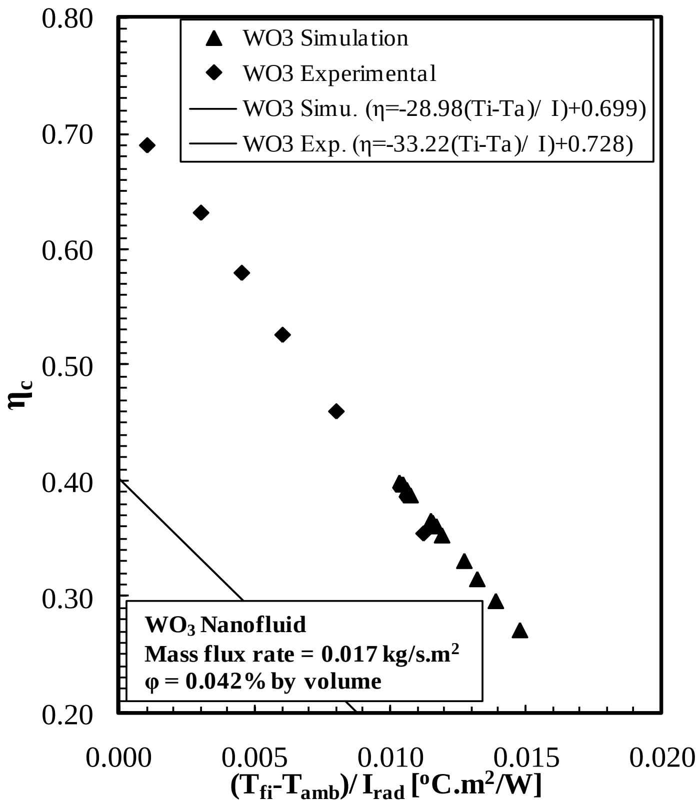

Fig. 2 Comparison between simulation results and experimental work for WO_3 water nanofluid

3.1 Performance of ETC using CeO_2/water

The results will be presented the performance of solar heating systemon14th February, 2019. This day is selected for this investigation because it is considered mid-winter season and a clear sky day.

The intensity of solar radiation in Cairo- Egypt on 14th February is shown in Fig.3. From this figure it can be seen that the intensity ofthe solar radiation increaseswith increasing daylight time. The solar radiation records the maximum value at 12:00 PM (985 W/m^2) and drops to low values for the rest of the day.

The difference of working fluid temperature through ETC is important parameter to give a clear picture of performance of solar heating system.Fig. 4 illustrates the variation of the temperature difference across the collector using CeO_2/waterat different concentrations.The temperature difference has the same trend of solar radiation intensity. Also, it can be seen that the water has the lowest temperature difference while the nanofluid has high values at 12:00 PM. The temperature difference is directly proportional to the increase in the concentration of nanofluids. For nanofluids concentration of 0.015%, 0.025%, 0.035% and 0.045%, the temperature differences are higher than water by 27.8%, 31.6, 33.7% and 35.6%; respectively. That is because the nano-particles increase the thermal conductivity.Fig. 5 shows the useful heat gain of ETC using CeO_2/water nanofluid and water during daylight time. For all nanofluid concentrations, the useful heat gain increases to the maximum value at 12:00PM.

DOI: 10.31695/IJASRE.2020.33698

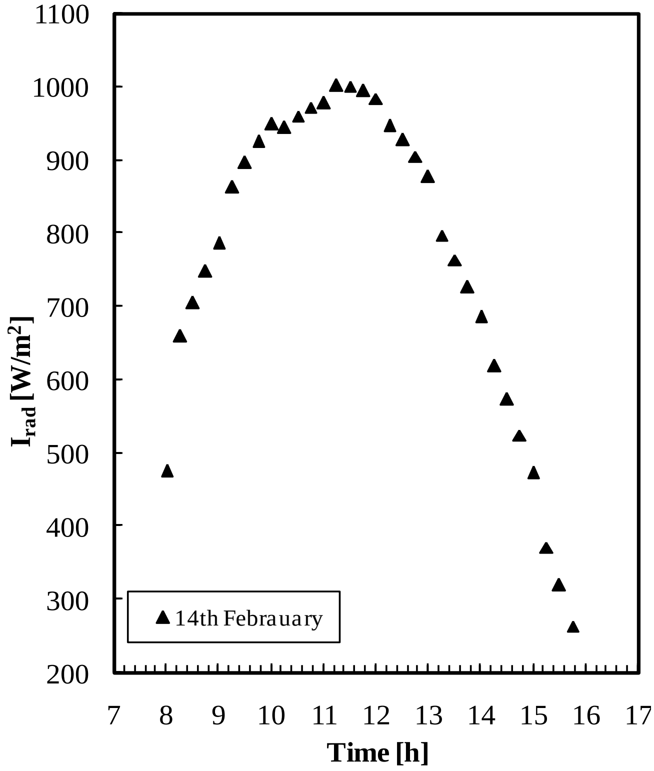

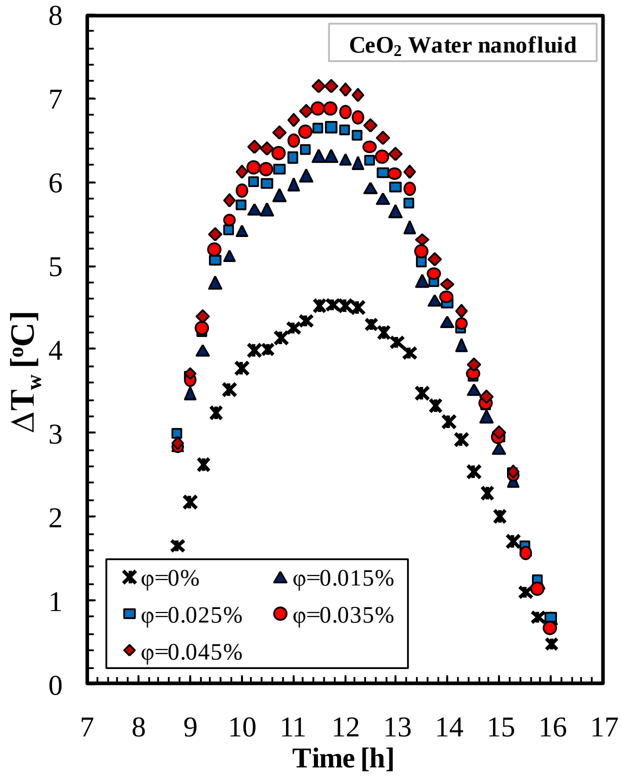

Fig.3 Solar radiation intensity through ETC with daylight time on 14th of February

Fig.4 ETC temperature difference with CeO_2 nanofluid at different concentrations versus water

Fig. 5 shows the useful heat gain of ETC using CeO_2/water nanofluid and water during daylight time. For all nanofluid concentrations, the useful heat gain increases to the maximum value at 12:00PM.The useful heat gains are707 W, 744 W, 767 W, 790 W and 526 W for concentrations of 0.015%, 0.025%, 0.035%, 0.045% and water; respectivelyat 12:00PM. That is result to the high temperature difference.

Fig.6 indicates the thermal efficiency of ETC using CeO_2nanofluid with different concentrations and water as working fluids. The thermal efficiency is high due to higher concentration of nanofluid compared to water. At 12:00 PM, the thermal efficiencyfor concentrations of 0.015%, 0.025%, 0.035% and 0.045% are increased by 25.7%, 29.3%, 31.5% and 34.2%; respectively, compared with the thermal efficiency of water.

DOI: 10.31695/IJASRE.2020.33698

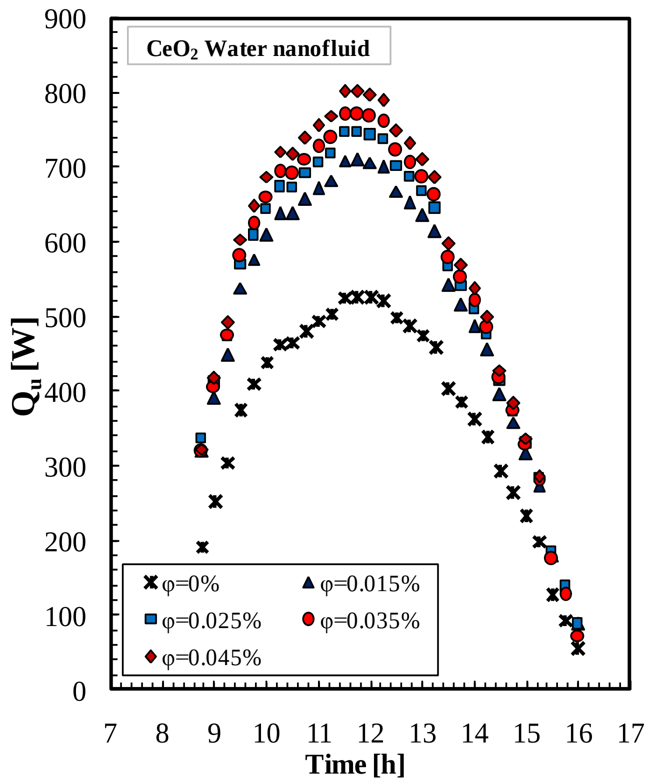

Fig.5 Useful heat gain by ETC with CeO_2nanofluid at different concentrations versus water

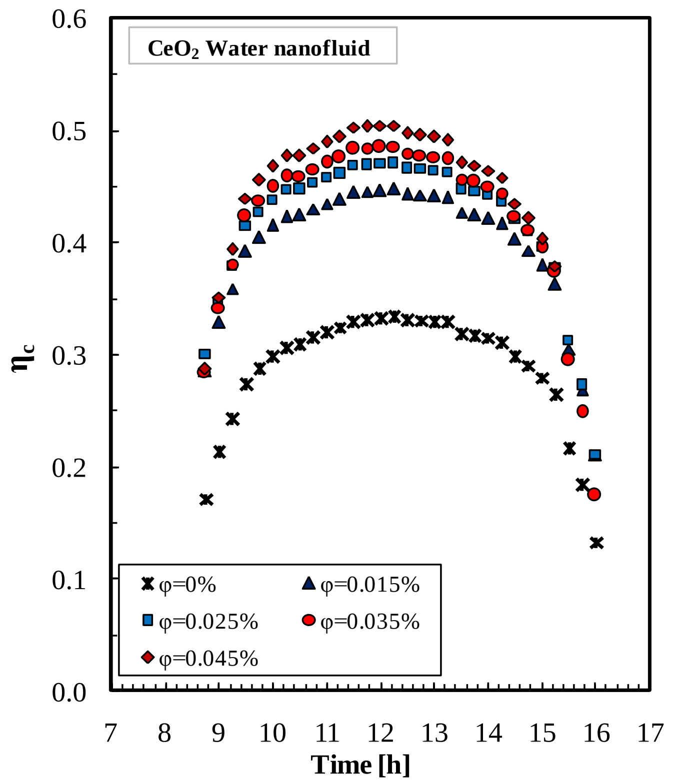

Fig. 6 ETC efficiency versus time for CeO_2nanofluid at different concentrations versus water

The optical efficiency $F_R(\tau\alpha)$ and energy losses coefficient $(-F_R.U_L)$ of ETC can be calculated from Eq.(10) [21]:

$$\eta_c = F_R\left(\tau\alpha\right) - F_R U_L\left(\frac{T_{f,i} - T_{amb}}{I_{rad}}\right) \qquad (10)$$

Table [3] illustrates the optical efficiency of ETC FR(τα) and energy losses coefficient $(-F_R.U_L)$ for CeO_2nanofluid. At [(Ti-Ta)/I] is equal to zero the thermal efficiency of the ETC gives a higher value. The thermal optical efficiency of CeO_2nanofluidincreases with increasing nanofluid concentration. The energy loss coefficients decrease when concentration is low.

Table [3]ETC optical efficiency and energy loss coefficients for CeO_2 with different concentrations

Working fluid	Optical efficiency $F_R(\tau\alpha)$	Energy losses coefficient $(-F_R.U_L)$[W/m^2.K]
Base water	0.471	15.08
0.015%	0.632	16.25
0.025%	0.682	17.87
0.035%	0.752	22.06
0.045%	0.813	24.83

3.2 Performance of ETC using WO_3/ water

This section discusses the performance of ETC usingwater and WO_3Nano fluidas working fluid. The nanofluid has volumetric concentrations of 0.015%, 0.025%, 0.035%, and 0.045%. The relation between the temperaturesdifferenceswith daylight time are illustrated in Fig. 7.As seen from this figure, the temperature differences of WO_3/water are high than that of base water. At 12:00 PM, the temperature difference are increased than that water by about 8.5%, 9.4%, 13.2% and 15.3%, at volumetric concentrations of 0.015%, 0.025%, 0.035% and0.045%;respectively.

Fig. 8 indicates the useful heat gain from ETC using water and WO_3/water during daylight time. For all concentrations of nanofluid WO_3/water, the useful heat gain reaches maximum value at 12:00PM. The useful heat gains increase with increasing

DOI: 10.31695/IJASRE.2020.33698

volumetric concentration. At volumetric concentration of 0.045% , the useful heat gains is higher than that of water by 1.14 times at 12:00PM. This also can be attributed to the high temperature difference.

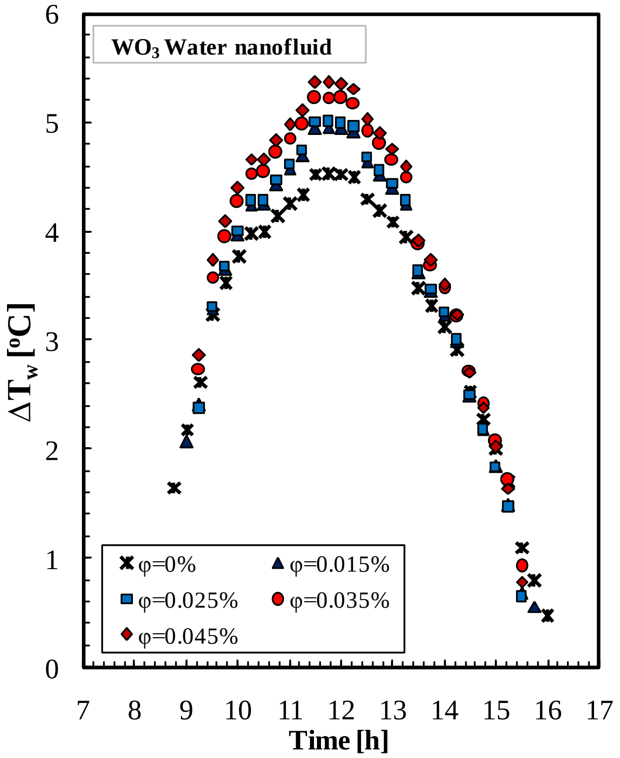

Fig.7 ETC temperature difference with WO_3 nanofluid at different concentrations versus water

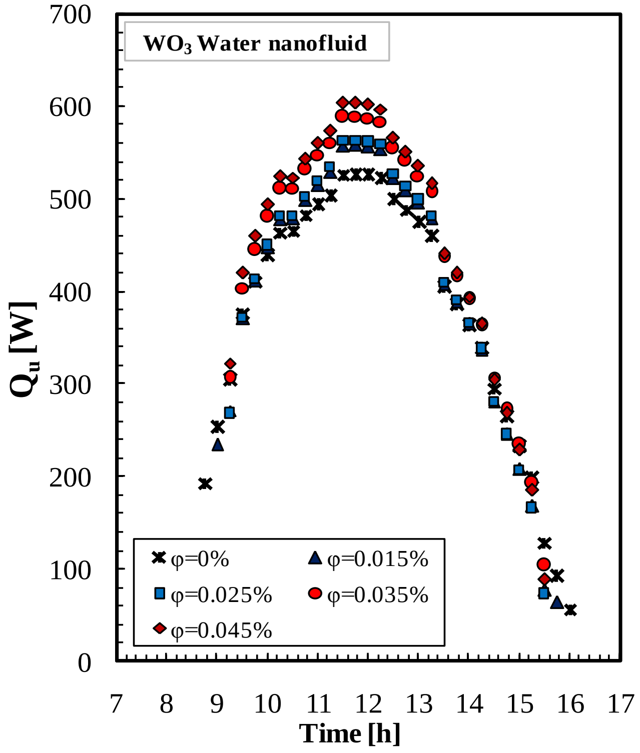

Fig.8 Useful heat gain by ETC with WO_3 nanofluid at different concentrations versus water

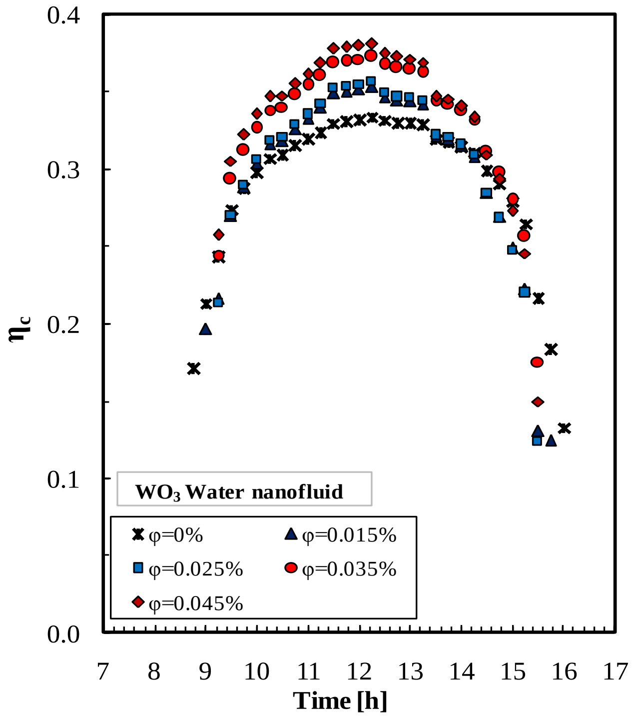

Fig. 9 ETC efficiency versus time for WO_3 nanofluid at different concentrations versus water

Fig. 9 demonstrates the thermal efficiency of ETC at different concentrations of WO3/water nanofluid. At certain time of 12:00 PM, the thermal efficiency of WO_3/water is higher than the thermal efficiency of water by 5.7%, 6.5%, 10.5 and 12.6%, at concentrations of 0.015%, 0.025%, 0.035%, and 0.045%; respectively.

The optical efficiency of ETC $F_R(\tau\alpha)$ and energy losses coefficient ($-F_R.U_L$) for WO_3/water are illustrated in Table [4]. The highest thermal optical efficiency and highest energy loss coefficient of ETC using WO3/water occur at 0.025% concentration.

DOI: 10.31695/IJASRE.2020.33698

Table [4]ETC optical efficiency and energy loss coefficients for WO_3 with different concentrations

Working fluid	Optical efficiency $F_R(\tau\alpha)$	Energy losses coefficient $(-F_R.U_L)$[W/m^2.K]
Base water	0.471	15.08
0.015%	0.595	26.45
0.025%	0.679	33.93
0.035%	0.636	26.74
0.045%	0.705	32.36

3.3 Performance of ETC using AL_2O_3/water

Fig. 10indicates the temperature difference through the collector using water and AL_2O_3/water nanofluid.The water has lowest temperature difference while the highest value can be achieved byAL_2O_3/water nanofluids. At 12:00 PM, the temperature differences of AL_2O_3/water arehigher than water by about 8%, 16.7%, 23.7% and 29.8% for a concentration of 0.015%, 0.025%, 0.035% and 0.045%; respectively.

The variation of useful heat gain from ETC using water and AL_2O_3/water nanofluid are shown in Fig. 11.With AL2O3 /water nanofluid, the useful heat gains have higher values than water. At 12:00PM, the useful heat gains are555 W, 613 W, 669 W and 727 W for concentrations of 0.015%, 0.025%, 0.035% and 0.045%; respectively while the useful heat gains of water is 526 W.

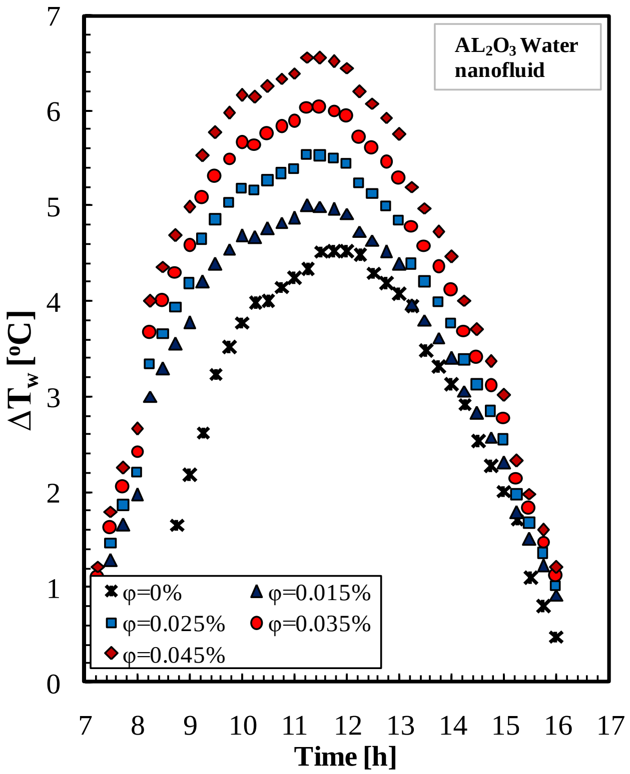

Fig.10 ETC temperature difference with AL_2O_3nanofluid at different concentrations versus water

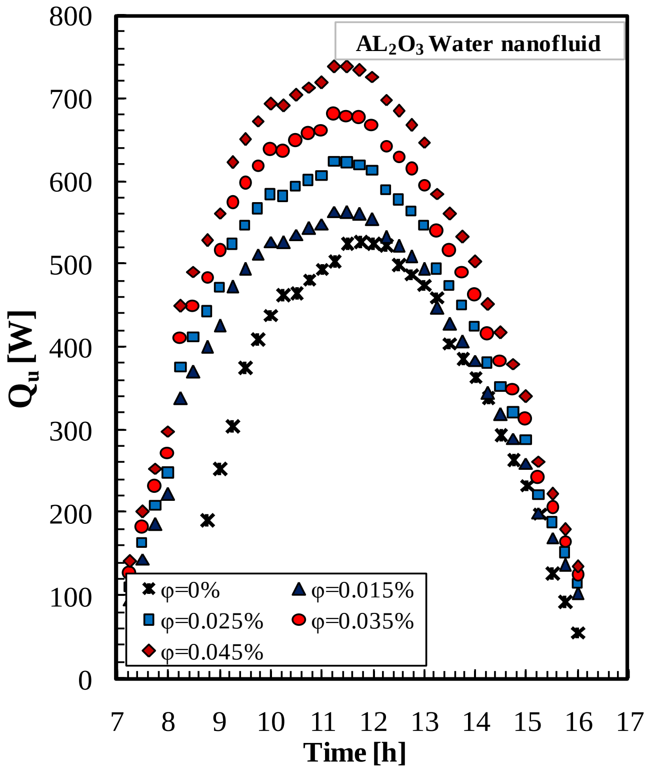

Fig.11Useful heat gain by ETC with AL_2O_3nanofluid at different concentrations versus water

DOI: 10.31695/IJASRE.2020.33698

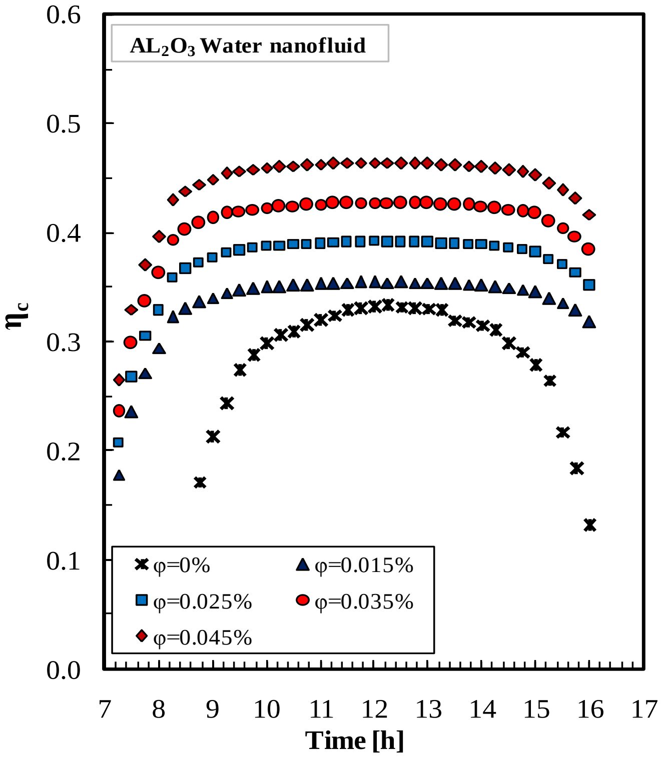

Fig. 12 ETC efficiency versus time for AL_2O_3nanofluid at different concentrations versus water

Fig. 12shows the thermal efficiency of ETC working with water and AL_2O_3/ water nanofluid. Thermal efficiency is directly proportional to the increased volumetric concentration. At 12:00 PM and at concentrations of 0.015%, 0.025%, 0.035% and 0.045%, the thermal efficiency is higher by 6.2%, 15.1%, 22.4% and 28.4%; respectively, compared with water.

The optical efficiency of ETC $F_R(\tau\alpha)$ and energy losses coefficient ($-F_R.U_L$) for AL_2O_3/ water nanofluid are illustrated in Table [5]. The thermal optical efficiency of AL_2O_3/ water nanofluid reaches to 0.447 at 0.045% concentrationwhereas the highest value of energy loss coefficient is 1.92 W/m^{2}K at concentration of 0.045%.

Table [5]ETC optical efficiency and energy loss coefficients for WO_3 with different concentrations

Working fluid	Optical efficiency $F_R(\tau\alpha)$	Energy losses coefficient ($-F_R.U_L$)[W/m^2.K]
Base water	0.471	15.08
0.015%	0.37	1.62
0.025%	0.41	1.73
0.035%	0.447	1.82
0.045%	0.487	1.92

3.4 Comparison between different nanofluids

This section will discuss ETC performance using different types of nanofluids. This comparison is conducted at 0.017 kg/m^{2}s mass flux rate and volumetric concentrationof 0.045%.

Fig. 13 illustrates the variation of the temperature difference across the collector using various nanofluids and water as working fluids. With nanofluids the temperature differences are higherthan the temperature difference of base water. At 12:00 PM, the temperature differences for CeO_2/water, AL_2O_3/water and WO_3/water nanofluids are 35.6%, 29.8% and 15.3% higher than water; respectively. That is because the thermal conductivity increases by nano-particles.

Useful heat gain from ETC with nanofluids compared with the water is showed in Fig. 14. For all working fluids, the useful heat gain increases to the higher value at 12:00PM. The useful heat gains of CeO2/ water, AL_2O_3/ water and WO_3/water nanofluids at 12:00PM are higher than water by 50.2%, 38.2% and 14.3%; respectively. This can be attributed to the high temperature difference.

DOI: 10.31695/IJASRE.2020.33698

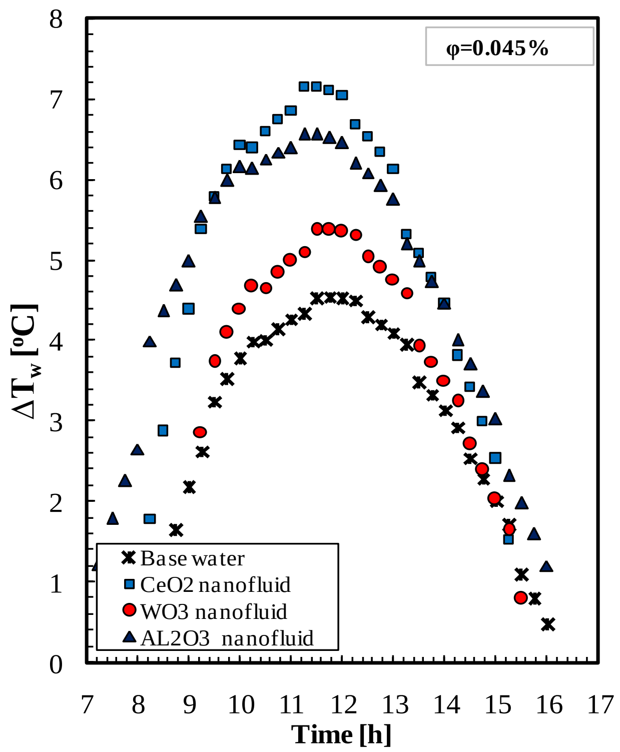

Fig.13 Temperature difference through ETC with different nanofluids and water

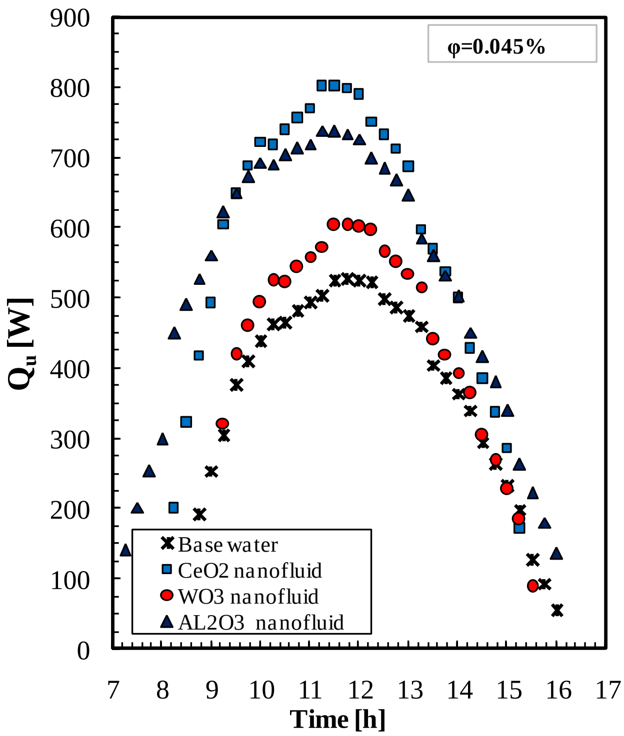

Fig.14 Useful heat gain by ETC with different nanofluids and water

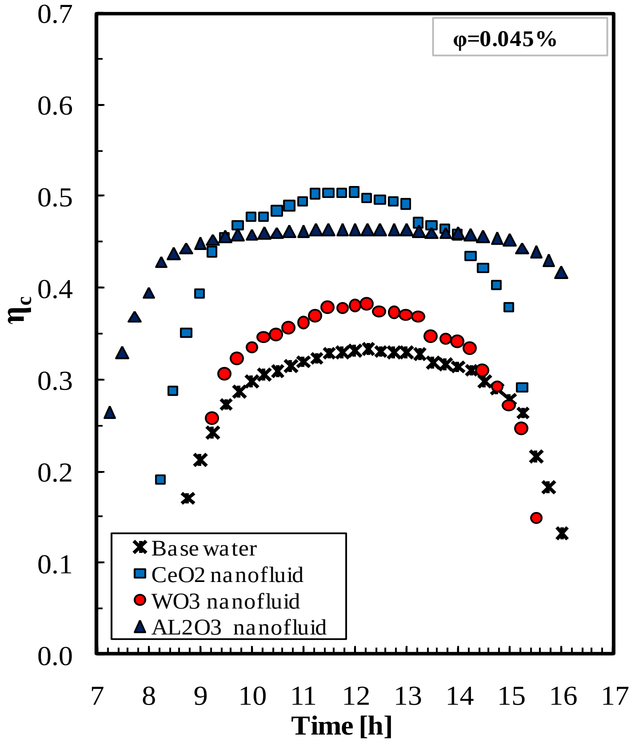

Fig. 15 ETC efficiency versus time for different nanofluids and water

Fig 15 shows the thermal efficiency of ETC using nanofluids and water as working fluids. The thermal efficienciesof CeO_2/ water, WO_3/ water and AL_2O_3/ water nanofluids are higher compared with the water at the same concentration. At 12:00 PM, the thermal efficiencies ofCeO_2/ water, AL_2O_3/ water and WO_3/ water nanofluids increase by 34.2%, 28.4% and 12.5%;respectively, compared with the thermal efficiency of water.

DOI: 10.31695/IJASRE.2020.33698

5. CONCLUSION

This paper presents theoretical study to investigate the performance characteristics of ETC using varied nanofluid types and different concentrations in weather data of Cairo – Egypton 14th February. The simulation is performed using water, CeO_2/ water, WO_3/ water and AL_2O_3/ water nanofluids as working fluids. From this simulation it can be concluded that:

1. Using water nanofluids, the performance of ETC is much higher compared with the water at study concentrations.
2. At concentration of 0.045%, the performance of ETC using CeO_2/ water nanofluid gives higher temperature difference and higher thermal efficiency by 35.6 % and 34.2%; respectively compared with the water.
3. At 12:00 PM and 0.045% nanofluid concentration, the temperature difference, useful heat gain and thermal efficiency of WO_3/water are increased by 15.3%, 14.3% and 12.6%; respectively, compared with water.
4. The temperature difference, useful heat gain and thermal efficiency ofAL_2O_3/water are higher than that waterby 29.8%, 38.2% and 28.4%; respectively,at 0.045% concentration.
5. For CeO_2 /water, the useful heat gain changes from 707W to 790 W when the concentration is varied from 0.015% to 0.045% at midday.
6. At 12:00 PM, the thermal efficiency of ETC using AL_2O_3/ water are increased than that of water by 6.2% and 28.4% when the concentrations are 0.015 and 0.045%; respectively.
7. The thermal optical efficiency of CeO2 nanofluid increases from 0.632 to 0.813 when nanofluid concentrations are 0.015 and 0.045%; respectively.

REFERENCES

[1] *B. Buonomo, F. Cascetta, L. Cirillo, S. Nardini*, 'Application of nanofluid in solar cooling system: Dynamic simulation by means of TRNSYS software', Modeling measurement and control B, vol. 87, pp. 143–150, 2018.

[2] *A Fathima, P. Sreekala, B. K. Mathew*, 'Performance analysis of solar thermal evacuated tube collector using different nanofluids', International journal of engineering science and research technology , vol. 5, pp. 367–373, 2016.

[3] *M. Asim, J. Dewsbury, S. Kanan*, 'TRNSYS simulation of solar cooling system for the hot climate of Pakistan', Energy procedia, vol. 91, pp. 702–706, 2016.

[4] *L. Ayompe, A. Duffy, S. McCormak, M. Conlon.,* 'Validated TRNSYS Model for Forced Circulation Solar Water Heating Systems with Flat Plate and Heat Pipe Evacuated Tube Collectors', Smart Grid and Renewable Energy vol. 31, pp. 1536–1542, 2011.

[5] *B. Yang, J. Liu, M. Hao, L. Gao,* 'Study on performance of solar water heating system using TRNSYS software' Chemical engineering transactions, vol. 70, pp. 2071–2076, 2018.

[6] *J. Fan, J. Dragsted, S. Furbo,* 'Validation of simulation models for differently design heat pipe evacuated tubular collector' Proceedings of ISES Solar world congress, pp. 663-668, 2007.

[7] *M. J. R. Abdunnabi, D. L. Loveday,* 'Optimization of thermosyphon solar water heaters using TRNSYS, Part1: Improved model development and validation' International conference on future environment and energy IPCBEE , vol. 22, pp. 145-153, 2012.

[8] *M. N. Mohammed, M. A. Alghoul, Kh. Abulqasem, A. Mustafa, Kh. Glaisa, P. Ooshaksaraei, M. Yahya, A. Zaharim, K. Sopain*, 'TRNSYS simulation of solar water heating system in Iraq', the 4th WSEAS international conference on Energy and development, environment, biomedicine, pp 153-156, dio:10.13140/2.1.1979.8724, 2011.

[9] *B. H. Ali, S. I. Gilani, H.H. Al-kayiem,* 'Investigation of evacuated tube collector performance at high temperature mode using TRNSYS simulation model', Applied mechanics and materials, vol. 465-466, pp. 155–160, 2014.

[10] *S. Mohasseb, A. Kasaeian*, 'Comparing the Performance of Flat Plate Collector and Evacuated Tube Collector for Building and Industrial Usage in Hot and Cold Climate in Iran with TRNSYS Software', Ninth International Conference on Engineering Computational Technology, Napoli, Italy, pp. 1-13, 2014.

[11] *G. Utham, S. M. Agravat, B. Jani, J. Bhutka*, 'Modelling, transient simulation and economic analysis of solar thermal based air conditioning system in Gujarat', Smart grid and renewable energy, vol. 7, pp. 233-246, 2016.

[12] *F. Assilzadeh, S.A. Kalogirou, Y. Ali, K. Sopain,* 'Simulation and optimization of a LiBr solar absorption cooling system with evacuated tube collector', Renewable energy, vol. 30, pp. 1143-1159, 2005.

[13] *G.S. Gill, A.S. Fung* 'Solar domestic hot water system analysis using TRNSYS', Fredricton, New Brunswick

[14] *S. A. Kalogirou, R. Agathokleous, G. Brone, A. Buonomano, C. Forzano, A. Palombo*, 'Development and validation of a new TRNSYS type for thermosyphon flat plate solat thermal collectors: energy and economic optimization for hot water production in different climates', Renewable energy, vol. 136, pp. 632–644, 2019.

[15] *M.J.R. Abdunnabi, k.M.A. Alakder, N.A. Alkishrwi, S.M. Abughres*, 'Experimental validation of forced circulation of solar water heating system in TRNSYS', Energy procedia, vol. 57, pp. 2477-2486, 2014.

[16] *F. Cao, L. Zhao, F. Zhang, L. Guo*, 'Redesign of water heating syatem using evacuated tube solar collectors: TRNSYS simulation and techno-economic evaluation', Heat transfer engineering, vol. 35(6-8), pp. 556–566, 2014.

DOI: 10.31695/IJASRE.2020.33698

[17] TRNSYS (2017) A Transient System Simulation Program, Version 17. University of Wisconsin- Madison-2017, http://sel.me.wisc.edu/trnsys/

[18] *Sharafeldin M. A., Gyula Grof* 'Evacuated tube solar collector performance using CeO_2 / water nano fluid', Journal of Cleaner Production, vol. 185, pp. 2–11, 2018.

[19] *Sharafeldin M. A., Gyula Grof* 'Efficency of evacuated tube solar collector using WO3/ water nanofluid', Renewable energy, vol. 134, pp. 453–460, 2019.

[20] *Javad G., Sidik N. A. C.* 'An experimental investigation on the effect of Al2O3/distilled water nanofluid on the energy efficiency of evacuated tube solar collector' International Journal of Heat and Mass Transfer, vol. 108, pp. 972-987, 2015.

[21] *ASHRAE Standard 93* 'Method of testing to determine the thermal of solar collector', Atlanta, GA, USA. 2003.

DOI: 10.31695/IJASRE.2020.33698